PAPER • OPEN ACCESS

Effect of aluminium substitution on low energy electrodynamics of barium-lead M-type hexagonal ferrites

To cite this article: Asmaa Ahmed *et al* 2019 *J. Phys.: Conf. Ser.* **1389** 012044

View the article online for updates and enhancements.

Effect of aluminium substitution on low energy electrodynamics of barium-lead M-type hexagonal ferrites

Asmaa Ahmed[1], Liudmila Alyabyeva[1], Victor Torgashev[2], Anatoly S Prokhorov[1,3], Denis Vinnik[4], Martin Dressel[1,5] and Boris Gorshunov[1]

[1] Laboratory of terahertz spectroscopy, Moscow Institute of Physics and Technology, Dolgoprudny, Russia

[2] Faculty of physics, Southern Federal University, Rostov-on-Don, Russia

[3] Prokhorov General Physics Institute of the Russian Academy of Sciences, Moscow, Russia

[4] South Ural State University, Chelyabinsk, Russia

[5] 1. Physikalisches Institut, Universität Stuttgart, Stuttgart, Germany

E-mail: a.gamal@phystech.edu

Abstract. We present the first detailed study of the terahertz-infrared dielectric response of single crystalline lead-substituted M-type barium hexaferrites doped with Al^{3+}. The broadband spectra of complex dielectric permittivity $\varepsilon^*(v)=\varepsilon'(v)+i\varepsilon''(v)$ of $Ba_{0.8}Pb_{0.2}Al_xFe_{12-x}O_{19}$ with concentrations of the dopant x(Al)=1.2, 3, 3.3 are obtained for two principle polarizations using Fourier-transform infrared spectroscopy and terahertz time-domain spectroscopy in the temperature range from 4 to 300 K and at frequencies from 10 cm^{-1} up to 8000 cm^{-1}. We observe a rich set of excitations and assign them to the electronic transitions within the ground state 5E of the 4-fold coordinated divalent iron and to phonon resonances. Effect of Al^{3+} cation substitution on low energy (terahertz) dielectric response and infrared phonon spectra of barium-lead M-type hexaferrites is analysed and discussed.

1. Introduction

In recent decades, great attention was paid to hexaferrites owing to their possible applications in electronics, magnetic memory storage, as materials for absorbing coatings, radiators, resonators, etc. A large class of hexaferrites with a general formula $MFe_{12}O_{19}$ (M=Ba, Pb, Sr, Ca, etc.) are called M-type hexaferrites and are structurally isomorphic to mineral magnetoplumbite. M-type hexaferrites exhibit a pronounced magnetocrystalline anisotropy, possess high Curie temperature (T_C~750 K), relatively high saturation magnetization (M_s~72 Am^2 kg^{-1}), high coercivity (H_c), residual magnetism (M_{rs}) and chemical stability [1].

Among the class, one of the most popular members is barium hexaferrite, $BaFe_{12}O_{19}$ (BaM), which is widely known as hard magnetic material with a coercivity of about 200 kAm^{-1}, high electric resistivity of $\approx$100 MΩcm and high magnetic and dielectric uniaxial anisotropy with respect to the crystallographic c-axis.

BaM has centrosymmetric structure with space group $P6_3/mmc$ and unit cell parameters $a=b=5.89$ Å and $c=23.17$ Å. The unit cell contains two molecules with thirty eight O^{2-} ions, two Ba^{2+} ions and twenty four Fe^{3+} ions that are combined into four blocks: two R-blocks $(BaFe_6O_{11})^{2-}$ and two S-blocks $(Fe_6O_8)^{2+}$ stacking along the main crystallographic axis in a sequence RSR^*S^* (* designates the

rotation by an angle 180° around the c-axis). The Ba^{2+} ions are located in the 12-fold oxygen environment, and the Fe^{3+} ions are distributed over five distinct site-positions with different coordination: in octahedral 2a, 12k and $4f_2$; in tetrahedral $4f_1$ and in trigonal bi-pyramidal (TBP) 2b. In the centrosymmetric structure, the trigonal bi-pyramidal Fe(2) ion must occupy the site at the local mirror plane of the polyhedron; however, it was shown that this position is unstable and favours the off-site shifts towards one of the two vertices of the TBP, and results in splitting of the 2b TBP into two 4e tetrahedra. Detailed discussions of the structural and physical properties of pure barium hexaferrite were presented in 1985 by Obradors et al. [2]. Also, magnetic and mechanical properties have been fully described and investigated in [3][4] [5].

Substitution of the crystal structure of BaM hexaferrites with additional elements by appropriate replacement of either M^{2+} or Fe^{3+} ions (or both of them, as in our case) can lead to giant change in their functional properties, such as coercive force, Curie temperature, magnetic permeability and dielectric permittivity. These substitutions open promising areas for practical applications in various fields of electronics, e.g., space telecommunication. Doping can also cause change in magnetic ordering, mechanical properties, unit cell parameters and dielectric response.

Magnetic properties of M-type hexaferrites and radio-frequency electromagnetic response with several dopants have been already focused on. At the same time, the infrared-terahertz electrodynamics is almost unexplored, even though terahertz frequencies are extremely promising from the standpoint of applications in microelectronics. Effect of substitution with Pb^{2+} is discussed in details in [6], [7].

In the present work, we present the first detailed investigation of low-energy (terahertz and far-infrared) dielectric response of single-crystalline barium hexaferrites doped with Pb^{2+} and Al^{3+} ions.

2. Experimental

Large high quality single crystals of lead-substituted BaM hexaferrites were grown by flux technique. We have studied the influence of Al doping on the dielectric response of $Ba_{0.2}Pb_{0.8}Al_xFe_{12-x}O_{19}$ with different concentrations of the dopant, $x(Al) = 1.2, 3$ and 3.3. Plane parallel slabs with a) the c-axis oriented normal to the slab surface and b) lying within its plane (sample thickness 100 ± 2 μm) were carefully prepared and polished which allowed us to measure the electrodynamic response for two principle polarizations, namely, with the electrical field vector E of the probing radiation oriented perpendicular to the c-axis and parallel to it.

A set of spectrometers was used to perform the measurements of broadband spectral response – spectra of real and imaginary parts of dielectric permittivity. A standard Fourier-transform spectrometer (Bruker Vertex 80v equipped with a microscope Hyperion 2000 and with cold finger cryostat) was used to measure the reflection coefficient $R(\nu)$ in the frequency range from 30 up to 8000 cm^{-1}. At lower frequencies, two commercial time-domain spectrometers (Tera K15 Menlo GmbH and TeraView TPS 3000) equipped with exchange gas cryostats were used to obtain the spectra of complex dielectric permittivity in the 10-100 cm^{-1} frequency range. The experiments were performed in a wide range of temperatures from 4 K to 300 K. Spectra were modelled using regular Lorentzian expression for the complex dielectric permittivity $\varepsilon^*(\nu)$ in order to describe the observed absorption resonances:

$$\varepsilon^*(\nu) = \varepsilon'(\nu) + i\varepsilon''(\nu) = \sum_j \frac{f_j}{\nu_j^2 - \nu^2 + i\nu\gamma_j} + \varepsilon_\infty \, , \qquad (1)$$

where $\varepsilon'(\nu)$ and $\varepsilon''(\nu)$ are real and imaginary parts of complex dielectric permittivity, $f_j = \Delta\varepsilon_j\nu_j^2$ is the oscillator strength of the j-th resonance, $\Delta\varepsilon_j$ is its dielectric contribution (dielectric strength), ν_j represents the resonance frequency, γ_j is the damping factor and ε_∞ is the high-frequency dielectric constant. Processing with the least square fitting the dielectric spectra together with the measured transmissivity $Tr(\nu)$ and reflectivity $R(\nu)$ spectra, we obtained broad band spectra of real and imaginary parts of dielectric permittivity of $Ba_{0.8}Pb_{0.2}Al_xFe_{12-x}O_{19}$ with different contents of Al^{3+}.

3. Results and Discussion

The infrared reflectivity spectra of $Ba_{0.8}Pb_{0.2}Al_3Fe_9O_{19}$ measured at room temperature for both principle polarizations are shown in figure 1. Rich sets of excitations are seen in the figure that corresponds to phonon resonances. The values of the high frequency permittivity, ε_∞= 5.6 and 4.24 for perpendicular and parallel polarizations, respectively, originating from electronic absorption processes were determined from the frequency independent high-frequency tails of the room temperature reflectivity spectra.

According to the factor group analysis, 17 E_{1u} and 13 A_{2u} modes are expected for the perpendicular ($E\perp c$) and parallel ($E\|c$) polarizations, respectively [8]. In the far-infrared region (90-1000 cm^{-1}), a set of polar phonon resonances was registered for both polarizations for all Al^{3+} dopant contents in the temperature range 4-300 K. For example, at T=300 K, in the spectra for the sample with x (Al) =3 we observed 10 E_{1u} polar modes for $E\perp c$ polarization and 8 A_{2u} polar modes for $E\|c$ polarization, for all studied samples. Comparing our results with those obtained for pure BaM [9], pure PbM [8] and mixed Ba-Pb substituted hexaferrites [10], we can say that we did not observe the expected numbers of resonances the possible reason being their broadening and slight shifts of resonance frequencies resulting from crystal field distortions induced by doping.
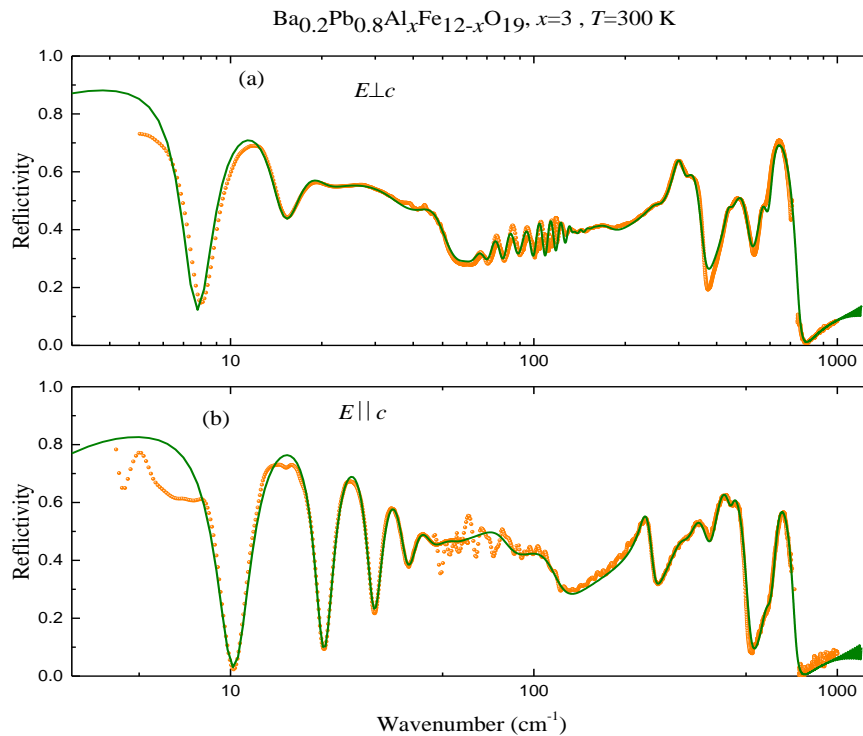

$Ba_{0.2}Pb_{0.8}Al_xFe_{12-x}O_{19}$, x=3 , T=300 K

Figure 1. Infrared reflectivity spectra of $Ba_{0.8}Pb_{0.2}Al_3Fe_9O_{19}$ single crystal measured at room temperature for two polarization $E\perp c$, panel (a), and $E\|c$, panel (b). Dots are experimental data; solid lines are theoretical modelling using least square fits with free Lorentzians, expression (1).

The terahertz spectra of the complex dielectric permittivity were measured at frequencies 10-100 cm^{-1} with a spectral resolution of 1.2 cm^{-1}. At terahertz frequencies, four absorption lines are resolved for the polarization $E\perp c$. Strong dependence of terahertz response on the temperature is clearly seen in figure 2 which shows the temperature dependence of dielectric contribution $\Delta\varepsilon$ and resonance frequency v for each absorption line (L1-L4) for the $Ba_{0.8}Pb_{0.2}Al_3Fe_9O_{19}$ compound. The observed excitations are assigned to electronic transitions between fine-structured components in the ground

state of divalent iron ions. In hexaferrites, there are several mechanisms of appearance of divalent iron, including defects, influence of crystal growth conditions and charge compensation [8], [10]. In lead-substituted hexaferrites, an additional mechanism applies. Pb^{2+} ions that have a lone electron pair on the outer electron shell share their 2 electrons via an exchange interaction and reduce the neighbouring trivalent iron to the divalent state [10]. The detected temperature evolution of the observed absorption lines indicates existence of a critical temperature that is associated with freezing out of dynamical oscillations of the iron ions within the split bi-pyramidal site-position [7].
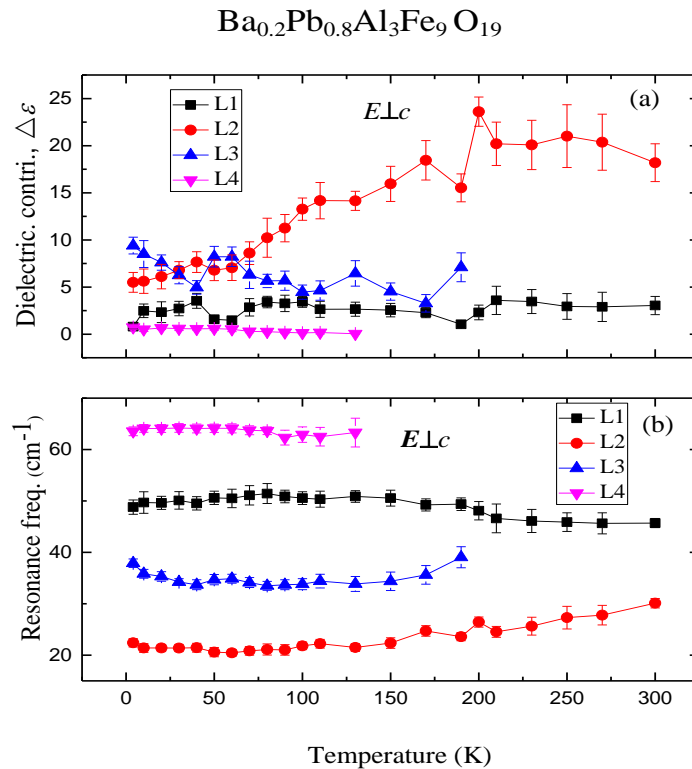
$$Ba_{0.2}Pb_{0.8}Al_3Fe_9O_{19}$$

Figure 2. Temperature dependence of the dielectric contribution $\Delta\varepsilon$ (a) and resonance frequency (b) of four observed absorption lines connected with the fine-structured Fe^{2+} ground state. Sample $Ba_{0.2}Pb_{0.8}Al_3Fe_9O_{19}$, polarization $E\perp c$.

The room temperature terahertz and infrared spectra of complex dielectric permittivity $\varepsilon^*(\nu)=\varepsilon'(\nu)+i\varepsilon''(\nu)$ of $Ba_{0.2}Pb_{0.8}Al_xFe_{12-x}O_{19}$ ($x=0$ [6], 1.2, 3, 3.3) for $E\perp c$ and ($x=1.2$, 3, 3.3) for $E\|c$ polarizations are shown in figure 3. We can say that chemical ionic substitution is considered as an effective tool to control the dielectric properties of Al^{3+} substituted barium-lead hexaferrites.

In figure 3 we show a comparison of complex dielectric permittivity (real part ε' and imaginary part ε'') spectra of barium lead substituted M-type hexaferrite (hereafter we will refer to this compound as "pure" meaning absence of Al ions) and compounds doped with Al^{3+}. From figure 3a, which represents spectra for perpendicular polarization $E\perp c$, we see that the real part of dielectric permittivity of doped compounds ($x=3$, 3.3) measured at 10 cm^{-1} is smaller by almost 20% than that of the pure compound ($x=0$). Moreover, at higher frequencies (>100 cm^{-1}), the doped compounds have significantly lower dielectric absorption than the pure one; for example, it changes significantly at around 300 cm^{-1} where the contribution from the phonon vibrations for the doped compound ($x=3.3$) is by about three times smaller than for the pure one.

In the doped compounds, the imaginary part of the dielectric permittivity for the $E\perp c$ polarization (figure 3b) slightly changes at frequencies >30 cm^{-1} with increase of Al concentration. Note that the

phonon resonances observed in pure compound above 100 cm^{-1} compound are much sharper than in doped ones indicating the distortions brought to the lattice by Al that leads to larger damping. However at lower frequencies (<20 cm^{-1}) the responses in the pure compound are more intensive than in the doped ones meaning that the intensity is suppressed by increase of the Al content.

On the other hand, as shown in figure 3c for the parallel polarization ($E\|c$), below 70 cm^{-1} the real part of the dielectric permittivity of the compound with the dopant content x=1.2 is larger than that in the compounds with higher concentrations (x=3 and 3.3).
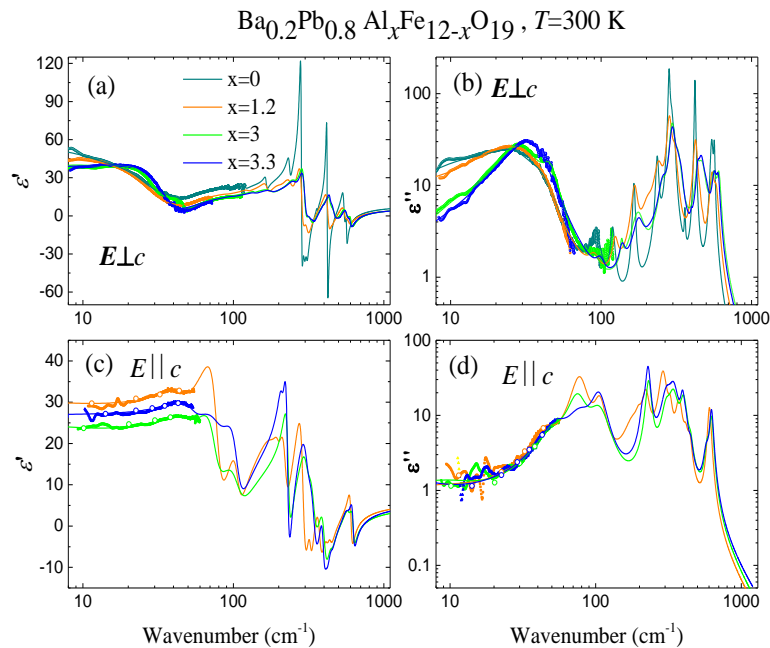

Figure 3. Spectra of real (a, c) and imaginary (b, d) parts of complex dielectric permittivity of Ba$_{0.2}$Pb$_{0.8}$Al$_x$Fe$_{12-x}$O$_{19}$ single crystal measured at T=300 K with orientation of the E-vector of the probing radiation perpendicular to the crystallographic c-axis ($E\bot c$, panels a, b) and along the c-axis ($E\|c$, panels c, d). Dots are experimental data; solid lines are theoretical data which show least square fits results obtained using Lorentzian expression (1). Open dots correspond to the data obtained at frequencies of interferometric maxima in transmission coefficient of the studied plane-parallel samples; at these frequencies the accuracy of determination of the dielectric parameters is highest.

However, the imaginary part of the permittivity for the parallel polarization (figure 3d) does not change significantly between all dopants all over the range. Thus, one can conclude that the presence of the Al^{3+} significantly changes low-energy dielectric response of the hexaferrite and can be used as an effective tool for tuning the low-energy dielectric characteristics of the material.

4. Conclusion

We have studied the effect of Al^{3+} cation substitution on terahertz-infrared dielectric response of barium-lead M-type hexaferrite, Ba$_{0.8}$Pb$_{0.2}$Al$_x$Fe$_{12-x}$O$_{19}$, with concentrations of the dopant x(Al)=1.2, 3, 3.3 and for two principle polarizations of the probing radiation relative to the crystallographic c-axis. The investigation of low-energy absorption and polar phonon resonances was performed using Fourier-transform infrared spectroscopy and terahertz time-domain spectroscopy at frequencies from 10 cm^{-1} up to 8000 cm^{-1} and in the temperature range from 4 to 300 K. We found that the presence of the Al^{3+} significantly changes the low-energy dielectric response of the hexaferrites: an increase of the aluminum content in the compounds leads to suppression of the terahertz absorption in comparison with pristine compound Ba$_{0.8}$Pb$_{0.2}$Fe$_{12}$O$_{19}$. We conclude that the dielectric response can be optimized

by appropriate replacement of Fe^{3+} ions with Al^{3+} ions and that this method can be considered as an effective tool for tuning the low-energy dielectric characteristics of the material.

Acknowledgments

References

[1]   Pullar R C 2012 *J. Prog. Mater. Sci*. **57** 7 1191–1334
[2]   Obradors X, Collomb A, Pernet M, Samaras D and Joubert J C 1985 *J. Solid State Chem*. **56** 171–181
[3]   Liu Y, Li Y, Liu Y, Yin HS, Wang L L, Sun K and Gao Y 2011 *Appl. Mech. Mater*. **69** 6–11
[4]   Wu M 2012 *Book of Advanced Magnetic Materials* **2** 12
[5]   Singh V P, Jasrotia R, Kumar R, Raizada P, Thakur S, Batoo K M and Singh M 2018 *World J. Condens. Matter Phys*.**8** 2 36–61
[6]   Alyabyeva L, Chechetkin A, Torgashev V, Zhukova E, Vinnik D, Prokhorov A, Gudkova S and Gorshunov B 2018 *43rd International Conference on Infrared, Millimeter, and Terahertz waves (IRMMW-THz)* 1-1
[7]   Alyabyeva L, Torgashev V, Zhukova E, Vinnik D, Prokhorov A, Gudkova S, Góngora D R, Ivek T, Tomi S, Novosel N, Starešini D, Jagli Z, Dressel M and Gorshunov B 2018 *43rd International Conference on Infrared, Millimeter, and Terahertz waves (IRMMW-THz)* 1-2
[8]   Zhukova E S, Mikheykin A S, Torgashev V I, Bush A A, Yuzyuk Yu I, Sashin A E, Prokhorov A S, Dressel M and Gorshunov B P 2016 *Solid State Sci*. **62** 13–21
[9]   Mikheykin A S, Zhukova E S, Torgashev V I, Razumnaya A G, Yuzyuk Y I, Gorshunov B P, Prokhorov A S, Sashin A E,. Bush A A and Dressel M 2014 *Eur. Phys. J. B* **87** 10 232
[10]   Alyabyeva L N, Torgashev V I, Zhukova E S, Vinnik D A, Prokhorov A S, Gudkova S A, Góngora D R, Ivek T, Tomić S, Novosel N, Starešinić D, Dominko D, Jagličić Z, Dressel M, Zherebtsov D A and Gorshunov B P 2019 *New J. Phys*. **21** 6 063016